Thermochimica Acta, 238 (1994) 277–293
Elsevier Science B.V., Amsterdam
SSDI 0040-6031(93)01875-F

Mathematical description of differential scanning calorimetry based on periodic temperature modulation

Bernhard Wunderlich *, Yimin Jin and Andreas Boller

Department of Chemistry, The University of Tennessee, Knoxville, TN 37996-1600 (USA) and *Division of Chemistry, Oak Ridge National Laboratory, Oak Ridge, TN 37831-6197 (USA)*

(Received 16 December 1993; accepted 24 January 1994)

Abstract

The changes needed in the mathematical description of differential scanning calorimetry caused by periodical modulation of temperature are presented. Calibration procedures and possible extensions of the method are suggested, all based on the model of scanning calorimetry without temperature gradient within the sample. The basic differential equation for heat flow under modulation conditions is solved and the steady state identified. The main advantage of modulated differential thermal analysis is the elimination of nonperiodic heat losses and gains. It is suggested that the precision of heat capacity measurement may be increased by a factor of 10 using proper calibration. The thermal analysis in transition regions is discussed.

1. INTRODUCTION

Modulated differential scanning calorimetry (MDSC) is a recent variation of differential scanning calorimetry (DSC) with constant heating or cooling rates. The first more detailed descriptions of MDSC were given at the 9th ICTA meeting in Hatfield, UK [1, 2]. An initial review of the method was given by Reading [3], who originally conceived MDSC and developed, in conjunction with TA Instruments, the well-known commercially available equipment [4]. The MDSC of TA Instruments is modulated at the block temperature $T_b(t)$ with a sinusoidally changing amplitude that is governed, as in standard DSC, by the temperature measured at the sample position

$$T_b(t) = T_0 + qt + A_{T_b} \sin \omega t \qquad (1)$$

where q is the underlying linear heating rate and T_0 is the initial isotherm at the beginning of the scanning experiment. The modulation frequency ω is equal to $2\pi/p$ in units of s^{-1}, with p representing the length of one cycle

* Corresponding author.

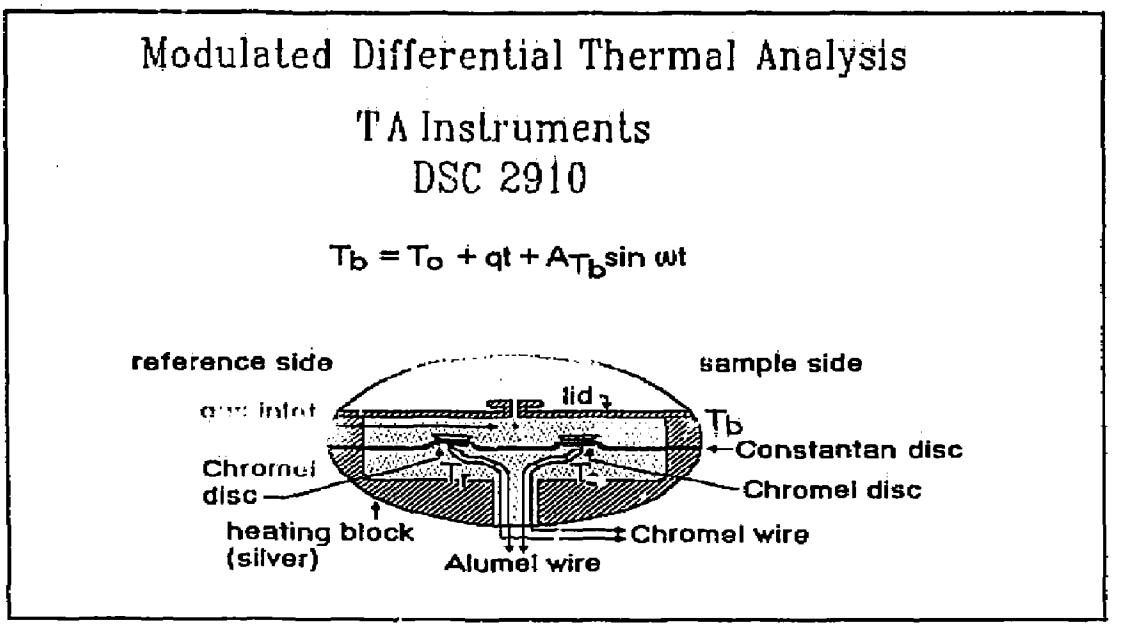

Fig. 1. Schematic diagram of an MDSC.

(s). Note that all variables and constants used in the equations are defined in more detail in Section 2. The reference sine wave of eqn. (1) thus adds a small sinusoidal component to the linear heating ramp qt. All phase lags of the periodic modulation are to be determined with reference to eqn. (1). Figure 1 shows a schematic diagram of the TA calorimeter cell with the positions where the various temperatures can be found. Similar modulation can be used with any of the other isoperibol scanning twin calorimeters which are described, for example, in refs. 5 and 6.

In this paper we discuss, based on a mathematical description, calibration procedures and heat capacity measurements. In an earlier paper [7], the experimental details and limits for measurement of heat capacity using the quasi-isothermal method, described in Section 4, have been evaluated for the instrument shown in Fig. 1 and need not be repeated. The influence of kinetic changes of the heat capacity, which may occur in the glass transition region, are now being investigated. The experimental results and kinetic analysis in the transition region will be published in due time [8]; a short discussion is given in Section 7. Slow changes due to chemical reactions, such as, for example, curing and the effect of oxidation of C_{70} at elevated temperature on the measurement of heat capacity [9], were found to be quantitatively eliminated as source of error when using MDSC. Similarly, heat leaks due to temperature drifts in the environment, or due to slow evaporation or sublimation that are common causes of error in DSC are eliminated as causes for error by the modulation. A more difficult problem to resolve is the treatment of the data of MDSC during phase transitions

involving large latent heats not far from the equilibrium or zero-entropy-production temperatures. In these cases the latent heats may be only partially reversing with the oscillating temperature because of the asymmetry of the melting and crystallization processes [10] or because the steady-state of the calorimeter is interrupted (see Sections 3 and 8). A detailed description of the influence of modulation for such transitions is in preparation, but is not yet available. Empirical descriptions are given, however, in refs. 1–3 and in many of the manufacturers' application briefs.

2. DEFINITION OF SYMBOLS USED AND LISTING OF OUTPUT PARAMETERS

For MDSC, variables and constants may have a somewhat different definition than for DSC. The listing that follows is sorted in order to use in the equations derived, starting with eqn. (1). Symbols with different subscripts are mostly to be found under the same entry, frequent subscripts are b for block, r for reference, s for sample, and Δ for difference.

$T(t)$ modulated temperature/K (or °C). For simplicity of the derivations we assume $T(t)$ is corrected for all instrumental parameters such as thermocouple effects and lags. Depending on the added subscript, T is the block, sample, or reference temperature (T_b, T_s, or T_r, respectively). The temperature difference $T_r - T_s = \Delta T$ is proportional to the measured heat flow $HF(t)$/W. As ΔT, HF is included in the calculations only after corrections.

T_0 temperature at time zero/K. At time zero it is usually assumed that $T_b = T_s = T_r = T_0$; furthermore for simplification of integrations, T_0 is sometimes taken to be zero.

q underlying heating rate/K min^{-1}. For quasi-isothermal measurements $q = 0$, for scanning experiments q is the linear change of temperature, disregarding the sinusoidal change in heating rate due to modulation ($dT/dt = q + A_{T_b}\omega \cos \omega t$).

t time/s.

A_T maximum amplitude of a modulated temperature/K. Maximum modulation amplitudes of the heater block temperature, sample temperature, and reference temperature are A_{T_b}, A_{T_s}, and A_{T_r}, respectively. The maximum amplitude of the temperature difference $T_r - T_s$ is A_Δ. It can be related to the maximum heat flow amplitude A_{HF} by an appropriate conversion factor with dimension W K^{-1} (note that $K_{C_p}A_{HF} \equiv KA_\Delta$).

$\omega = 2\pi/p$ modulation.

p period of one cycle/s.

ωt reference sine wave angle/rad. This is the sinusoidal modulation against which all phase lags are determined (see eqn. (1)).

$C_p(t)$ heat capacity at constant pressure, usually given per mole of material/J K^{-1} mol^{-1}. For the calorimeter as a whole, the heat capacity is measured in J K^{-1}, C_r is the heat capacity of the reference calorimeter and C_s is the heat capacity of the sample calorimeter. When using an empty pan as reference $C_r = C'$ and the heat capacity of the sample calorimeter C_s is then (when used with an identical pan as the reference calorimeter) $mc_p + C'$, where m is the sample mass/g and c_p is the specific heat capacity/J K^{-1} g^{-1} of the sample.

Q heat added/J. As before, subscripts are added to designate heat added to the sample (Q_s) or reference (Q_r) (both are zero at $t = 0$).

K Newton's law constant/J s^{-1} K^{-1}. To simplify the calculations K is assumed to be identical to sample and reference calorimeters. Note that the modulation time is usually given in seconds, while linear heating rates are often given in minutes. In the latter case the dimension of K must be changed appropriately.

K_{c_p} heat capacity calibration constant; it is dimensionless. Used for the calculation of the reversing part of the heat capacity in MDSC.

ε, ϕ, δ, Φ phase shifts of the modulation (phase angles)/rad, relative to the modulation phase at the block temperature (see eqn. (1)). The phase angles ε, ϕ, and δ refer to T_s, T_r, and ΔT; Φ is the experimentally determined difference $\varepsilon - \delta$.

Next, it is of interest to summarize how some of the experimental data are extracted from the experiment. Figure 2 illustrates in the upper sketch the phase-shifted temperature T_s. The bottom graph illustrates how the modulation of T_s can be separated into one part that is in-phase with T_b (component described with sin ωt), and another that is out-of-phase (component described with cos ωt). The sum is given at the bottom of the graph (for q and $T_0 = 0$) and described in detail in Sections 3 (eqns. (6) and (6a)) and 4 (eqn. (10)). Similar curves can be drawn for T_r and ΔT. The first job is then to extract the effect of the modulation from the recorded signals. This can be accomplished by a Fourier transform or deconvolution of the reversing part of the signal. Note that the oscillating part of the signal averages to zero when integrated over a complete cycle. In practice, the deconvolution is done by continued integration, averaging and smoothing over several cycles, indicated by the average symbol $\langle\ \rangle$. A typical output at the time t_n is

Heat capacity

$$C_p(t_n)[= K_{c_p} \times \langle A_{/\!/}(t_n)\rangle / (\langle A_T(t_n)\rangle \times \omega]/\text{mJ K}^{-1}$$

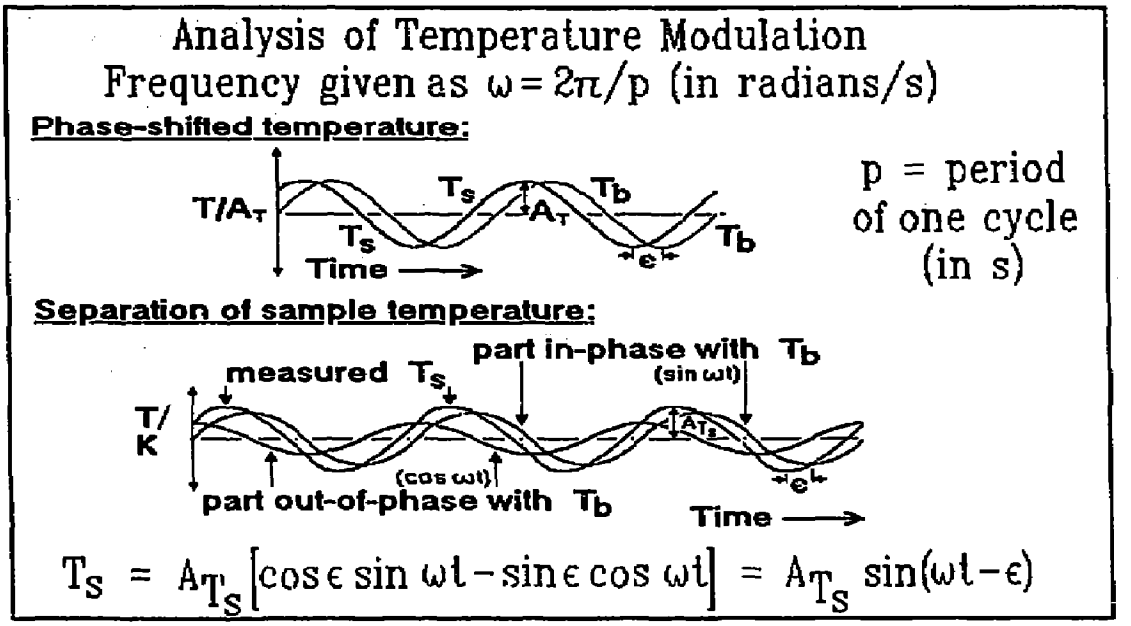

Fig. 2. The modulation of temperature. The upper sketch represents the phase-shifted temperature T_s relative to themodulated block temperature T_b, the latter being represented by eqn. (1). Both curves are shown after subtraction of $T_0 + qt$, and are plotted in normalized dimensionless temperature units of T/A_T.

Reversing heat flow

$C_p(t_n) \times \langle q(t_n)\rangle$/mW

(If heat flow is recorded with the endothermic (positive) direction downwards (as, for example, in the TA Instruments MDSC), one must multiply C_p by -1.)

Nonreversing heat flow

$\langle HF(t_n)\rangle - C_p(t_n)\langle q(t_n)\rangle$/mW

(Multiply C_p by -1 if heat flow is recorded with the endothermic direction downwards.)

Phase

$\langle \Phi(t_n)\rangle$/rad

For on-line observation, the data are available only a certain time after measurement because of the delay caused by the deconvolution and smoothing. The heat capacity is first evaluated from the modulation of ΔT and T_s, as expressed by the maximum amplitudes as described, for example, by eqns. (21)–(24). Next, the reversing heat flow is computed by multiplication of the heat capacity with the heating rate q. The nonreversing heat flow is, finally, computed by subtracting the reversing heat flow from the total heat flow (the latter is identical to the result from standard

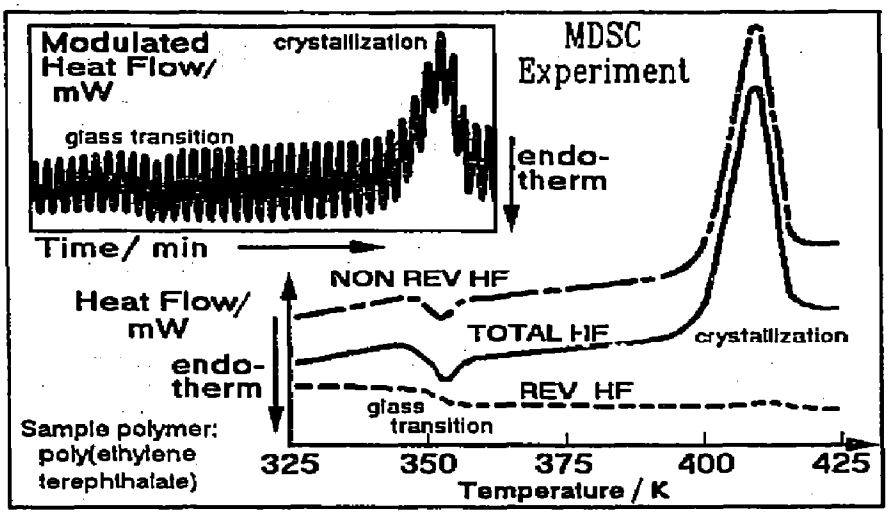

Fig. 3. Example output of an MDSC experiment on poly(ethylene terephthalate) [4]. The insert in the upper left shows the modulated heat-flow amplitude ($q = 5$ K min^{-1}, $p = 2$ min, $A_{T_s} = 7.5$ K). Note the elimination of the enthalpy relaxation at the glass transition and the heat of crystallization from the heat capacity (REV HF).

DSC). In principle, this nonreversing heat flow is, thus, the base line for the determination of the reversing heat capacity. Figure 3 shows an example of an experimental output.

At this point one may ask the question: is MDSC worth the additional effort (and expense)? Normal DSC can also measure heat capacity, namely by subtraction of a suitable, previously determined base line, and calibration with runs using an empty pan and a sapphire standard [5]. Using a three-position DSC (triple calorimeter) it is even possible to compress the heat capacity measurement into a single run [11]. Why then measure C_p with a new modulation method and then subtract it from the total heat flow to get a base line that is not needed anymore for heat capacity measurement? The answer can be given in two parts. First, the modulation gives a better precision in heat capacity. We estimate that for equal masses the precision may be higher by as much as a factor 10 [7]. All error signals of frequencies other than ω are eliminated. Second, the nonreversing signal may contain important information on irreversible processes, such as slow chemical reactions (oxidation, curing, evaporation, etc.) and nonequilibrium phase transitions (crystallization and reorganization); it may even enable us to separate the complicated simultaneous fusions, glass transitions, and annealings, common in many macromolecules. All this certainly makes for a more powerful technique, that may well be called the greatest advance in DSC since its inception some 35 years ago. It also gives an incentive to make a special effort to understand the theory behind the technique and to establish its limits.

The phase angle is also listed as an experimentally available parameter.

It could also be used for different data interpretation as will be shown in Section 6. Up to now, it seems, however, more advantageous to use the maximum amplitudes A for measurement of heat capacity.

3. THE STEADY STATE

First, it will be shown that a sample in a location separated by a thermal resistance from a heat reservoir that changes its temperature T_h as indicated in eqn. (1) will reach a steady state that changes in temperature with the heating rate q and contains a phase-shifted temperature oscillation of the same frequency ω as the reservoir (heater block of Fig. 1). The maximum amplitude A_T, the heating rate q, and the heat capacity C_p are, for the present derivation, assumed to be constant with time and temperature. The basic condition for the following derivation is to have only negligible temperature gradients within the sample and reference, so that all heat flow is governed by the thermal resistance outside the sample and reference calorimeters, as contained in K. These conditions are the same as commonly set for DSC [5]. Newton's law of cooling is then, as usual

$$\frac{dQ}{dt} = K[T_h(t) - T(t)] \tag{2}$$

With the insertions for

$Q = C_p[T(t) - T_0]$ (remember $Q_0 = 0$)

$T(t) = (Q/C_p) + T_0$

and

$T_h(t) = T_0 + qt + A_{T_h} \sin \omega t$

one can obtain the differential equation for heat flow

$$\frac{dQ}{dt} = K\left[qt + A_{T_h} \sin \omega t - \frac{Q}{C_p}\right] \tag{3}$$

The solution of this differential equation can be found in any handbook (and checked by carrying out the differentiation suggested by eqn. (3))

$$Q = qC_p\left[t - \frac{C_p}{K}(1 - e^{-K/C_p})\right] + \frac{KA_{T_h}}{\left(\frac{K}{C_p}\right)^2 + \omega^2}\left[\left(\frac{K}{C_p}\right)\sin \omega t - \omega \cos \omega t + \omega e^{-K/C_p}\right] \tag{4}$$

At sufficiently long time, a steady state is reached ($Kt \gg C_p$) and eqn. (4) reduces to

$$Q = qC_p t - \frac{qC_p^2}{K} + \frac{KA_{T_h}}{\left(\frac{K}{C_p}\right)^2 + \omega^2}\left[\left(\frac{K}{C_p}\right)\sin \omega t - \omega \cos \omega t\right] \tag{5}$$

Division of eqn. (5) by C_p gives the expression for the steady state temperature $T(t) - T_0$

$$T(t) - T_0 = qt - \frac{qC_p}{K} + \frac{A_{T_h}\left(\frac{K}{C_p}\right)}{\left(\frac{K}{C_p}\right)^2 + \omega^2}\left[\left(\frac{K}{C_p}\right)\sin \omega t - \omega \cos \omega t\right] \tag{6}$$

Equation (6) can be used to compute both T_s and T_r by insertion of the heat capacities C_s and C_r, respectively. It represents the basic equation for calorimetry by heat flow. The first two terms on the right-hand side represent the temperature lag due to heat capacity and heating rate in a linearly heated calorimeter. The last term gives the modulation effect. It is also dependent on heat capacity, and instead of being heating-rate dependent, it is modulation-frequency and maximum-amplitude dependent. As remarked above, both parts of eqn. (6) can thus be used for C_p measurement.

Next, a phase angle can be introduced (ε for the sample temperature T_s (control position), and ϕ for the reference temperature T_r). Since $\sin^2 \varepsilon + \cos^2 \varepsilon = 1$, the following relationships can be extracted from eqn. (6) *:

$$\varepsilon = \arcsin \frac{\omega}{\sqrt{\left(\frac{K}{C_s}\right)^2 + \omega^2}} \tag{7}$$

$$\varepsilon = \arccos \frac{\frac{K}{C_s}}{\sqrt{\left(\frac{K}{C_s}\right)^2 + \omega^2}} \tag{8}$$

$$\tan \varepsilon = \frac{\omega C_s}{K} \tag{9}$$

* One can check that eqns. (7) and (8) are correct and useful by insertion into eqn. (6):

$$T_s - T_0 = qt - (qC_p/K) + A_{T_h} \cos \varepsilon(\cos \varepsilon \sin \omega t + \sin \varepsilon \cos \omega t) \tag{6a}$$

Note that $A_{T_h} \cos \varepsilon = A_{T_s}$, and that the trigonometric functions can be simplified by using the addition theorems (see eqns. (11) and (12)).

Furthermore, because $A_{T_h}\cos\varepsilon = A_{T_s}$ and $A_{T_h}\cos\phi = A_{T_r}$, and using the addition theorems of trigonometric functions ($\cos\beta\sin\alpha \pm \cos\alpha\sin\beta = \sin(\alpha \pm \beta)$), eqn. (6) can finally be rewritten as

$$T_s - T_0 = qt - \frac{qC_s}{K} + A_{T_s}\sin(\omega t - \varepsilon) \tag{10}$$

and

$$T_r - T_0 = qt - \frac{qC_r}{K} + A_{T_r}\sin(\omega t - \phi) \tag{11}$$

Equations (10) and (11) can now be used to express the temperature difference (or heat flow) signal of the MDSC. The derivation follows the derivation of the equations for standard DSC as given, for example in ref. 5, Section 4.4.2.

4. EQUATIONS FOR QUASI-ISOTHERMAL HEAT CAPACITY MEASUREMENT

For the measurement of heat capacity under practically isothermal conditions ($q = 0$) use can be made of the oscillating temperature T_s and temperature difference ΔT. The general equations of steady-state temperature difference can be derived from eqn. (2) by substituting temperature for Q, assuming that the heat capacity is constant over the amplitude of temperature oscillation

$$T_r - T_s = \frac{(C_s - C_r)}{K}\frac{dT_s}{dt} - \frac{C_r}{K}\frac{d(T_r - T_s)}{dt} \tag{12}$$

Equation (12) is derived by subtracting the expressions for $T_s - T_b$ from the analogous expressions for $T_r - T_b$ resulting from eqn. (2), and adding and subtracting $(C_r/K)(dT_r/dt)$. To simplify the calculations, the oscillating temperature T_s and temperature difference ΔT can be inserted into eqn. (12) as complex expressions *

$$T_s = A_{T_s} i e^{i(\omega t - \varepsilon)} \tag{13}$$

$$T_r - T_s = \Delta T = A_\Delta i e^{i(\omega t - \delta)} \tag{14}$$

$$A_\Delta e^{i(\omega t - \delta)} = \frac{(C_s - C_r)}{K} A_{T_s} i\omega e^{i(\omega t - \varepsilon)} - \frac{C_r}{K} A_\Delta i\omega e^{i(\omega t - \delta)} \tag{15}$$

$$e^{-i(\varepsilon - \delta)} = -\frac{KA_\Delta i}{A_{T_s}\omega(C_s - C_r)} + \frac{A_\Delta C_r}{A_{T_s}(C_s - C_r)} \tag{16}$$

* Using $\sin\theta \pm i\cos\theta = \pm i\, e^{\mp i\theta}$, the more common $\cos\theta \pm i\sin\theta = e^{\pm i\theta}$ differs from the expression used here by a phase shift of $\pi/2$, necessary since the initial condition at time zero is $T_s = T_r = T_h = T_0$ and $\Delta T = 0$.

By equating the imaginary and the real parts on both sides of eqn. (16), one finds

$$\sin(\varepsilon - \delta) = \sin \Phi = \frac{KA_\Delta}{A_{T_s}\omega(C_s - C_r)} \tag{17}$$

$$\cos(\varepsilon - \delta) = \cos \Phi = \frac{A_\Delta C_r}{A_{T_s}(C_s - C_r)} \tag{18}$$

Equations (17) and (18) are linked to the experiment via measurement of Φ (see Section 2). Furthermore, since $\sin^2 \Phi + \cos^2 \Phi = 1$, one can derive an expression for the heat capacity

$$1 = \left(\frac{KA_\Delta}{A_{T_s}\omega(C_s - C_r)}\right)^2 + \left(\frac{A_\Delta C_r}{A_{T_s}(C_s - C_r)}\right)^2 \tag{19}$$

$$(C_s - C_r) = \frac{A_\Delta}{A_{T_s}} \sqrt{\left(\frac{K}{\omega}\right)^2 + C_r^2} \tag{20}$$

Equation (20) leads to a particularly simple expression for the heat capacity C_s, if C_r is zero, i.e. if no empty pan is placed on the reference side of the DSC ($C_r \approx 0$). The measured C_s is, as usual, the heat capacity of the sample mc_p, plus the heat capacity of the empty pan C_p'. The heat capacity of sample and pan is then

$$C_s = \frac{KA_\Delta}{A_{T_s}\omega} \tag{21}$$

This equation compares to the exmperimental output given in Section 2.

For the case of an empty pan (identical to the sample pan) on the reference position, the calibration equation takes the form

$$mc_p = \frac{A_\Delta}{A_{T_s}} \sqrt{\left(\frac{K}{\omega}\right)^2 + C'^2} \tag{22}$$

i.e. in this case the overall calibration is dependent not only on the frequency of modulation, but also on the heat capacity of the empty reference pan.

Switching reference and sample pans, so that the control-thermocouple is on the reference side (the side of the empty pan or without pan), is a useful technique when working without modulation. Under such conditions the recorded temperature T_r is proportional to time t, even through transitions, giving the recorded T versus ΔT area proportionality to heats of transition (base-line method) [5]. In the case of modulation, the calibration with control of the reference calorimeter is, however, more difficult

$$(C_r - C_s) = \frac{A_\Delta}{A_T} \sqrt{\left(\frac{K}{\omega}\right)^2 + C_s^2} \tag{23}$$

Note that in eqn. (23) A_T refers to control at the reference side, i.e. it is in the prior notation A_{T_r}. For the condition that $C_r \ll C_s$, the sample heat capacity is equal to

$$C_s = mc_p + C' = \frac{K}{\omega} \frac{A_\Delta}{\sqrt{A_T^2 - A_\Delta^2}} \tag{24}$$

If, in addition $A_\Delta \ll A_T$, eqn. (24) reverts back to the simple calibration equation (eqn. (21)).

The measurement of heat capacity is now rather simple. The temperature range of interest is divided into, typically, 10 K intervals and the MDSC is programmed after an isotherm of about 3 min to measure at each temperature the heat capacity for, let us say, 10 to 30 cycles of oscillation. A 300 K temperature range can thus be covered overnight, leaving the daytime operation for faster nonisothermal MDSC or DSC applications. A complete heat capacity analysis would consist of (perhaps three) measurements of C_s, and a measurement of a calibration standard, such as sapphire, to be able to eliminate K at each temperature (at the chosen amplitude and modulation frequency). It is advisible to check how often the calibration must be repeated, i.e. how stable is the MDSC. Sequential measurement and calibration is initially advisable, followed by increasing the calibration interval as experience on the instrument stability is gathered. Examples of such measurements are given in ref. 7. By continuous operation it should thus be possible to completely characterize one to two samples per week, or 100 per year without interrupting daytime work. The complete literature on polymers does, however, at present contain no more than 100–200 such characterizations!

5. EQUATIONS FOR NONISOTHERMAL HEAT CAPACITY MEASUREMENT

The deconvolution of the experimental signal (see Section 2) separates the oscillating portion of the signal from the total average using several cycles of modulation. The oscillating part can be used, as before, for the measurement of heat capacity (reversing mode). The (smoothed and averaged) total heat flow is linked to the first parts of eqns. (10) and (11) (the part free of trigonometric functions). (Note that the oscillations give positive and negative contributions that average to zero for every complete cycle.) A full treatment of its relationship to heat capacity is available in the descriptions of standard DSC [5]. In principle, the heat capacity can thus be extracted from both, the oscillating (reversing) and the total signal [3], as discussed in Section 2. The total, averaged temperature difference is, again, given by eqn. (12). The common DSC analysis is in this case carried out by assuming that at steady state q can be equated to dT_r/dt (i.e. $dt = dT_r/q$). If

furthermore, the thermal analysis is carried out such that $C_s = mc_p + C'$ and $C_r = C'$, eqn. (12) simplifies to

$$mc_p = K\Delta T/q + [(K\Delta T/q) + C']\, d\Delta T/dT_s \quad (25)$$

Only if the actual baseline is close to horizontal, so that $d\Delta T/dT_s \approx 0$, is the heat capacity of the sample easily assessed as $K\Delta T/q$ (by analogy to eqn. (21)). Under all other circumstances the recording of ΔT (or HF) misses a certain portion of the heat capacity due to the fact that sample and reference calorimeter do not change their temperature with the same rate ($d\Delta T/dT_s \neq 0$). Fortunately the error is usually small (about 1% for 45° slopes if the sensitivity of recording ΔT is 100 times that of T). This error could easily be corrected because the term in brackets is approximately equal to the heat capacity ($C_s = mc_p + C'$), but to our knowledge it has not been done, except in software generated in our laboratory [11].

In contrast to the normal DSC, one finds that the heat capacity extracted from the modulation (MDSC, eqns. (21)–(24)) gives a precise representation, as in the isothermal heat capacity measurement described in Section 4. Care must be taken, however, to carry out the proper calibration, as discussed above. The advantages of MDSC thus lie not only in the elimination of any slow drifts of the calorimeter and irreversible processes in the sample, but also in the direct ability to link the measured ΔT to heat capacity.

The nonreversing part of the thermal analysis, obtained by subtracting the reversing part from the total (see Section 2), is naturally only approximately represented by $\langle HF(t)\rangle - C_p(t)\langle q\rangle$ because it still contains the effect from the difference between sample and reference heating rates on heat capacity. To make the small correction, eqn. (25) can be used. Frequently, however, the nonreversible heat capacity is only used as baseline for a heat of transition measurement. If these heats are more than one order of magnitude larger than the change in enthalpy caused by the change in heat capacity over the same temperature range, this correction should be negligible.

6. PHASE ANGLES

A comment must be made about the interpretation of the phase angles. Equation (9), for example, shows that simple calorimetry (commonly known as AC calorimetry) is possible making use of the sample calorimeter only (i.e. not using twin or triple calorimetry). The phase angle ε, if it could be determined with sufficient precision, would give a measure of heat capacity of the sample (without need to analyze the differential heat flow). The reference calorimeter, in turn, can supply via the phase lag ϕ the heat

capacity of the empty pan. If C_r is set experimentally, as usual, to be C', one can most easily obtain the heat capacity of the sample

$$(C_s - C_r) = \frac{K}{\omega}(\tan \varepsilon - \tan \phi) \tag{26}$$

$$mc_p = \frac{K}{\omega}(\tan \varepsilon - \tan \phi) \tag{27}$$

In case a three-position DSC cell is available (TA DSC cell 912), single-run DSC can be performed by using the third position for determining the phase lag for a calibration sample such as sapphire (Al_2O_3) contained in, again, an aluminum pan identical to the empty reference pan of heat capacity C'. Single run heat capacity measurement without modulation with the TA 912 cell was developed in our laboratory [11], as mentioned above, and could be improved by adding the modulation capability.

Again the question must be asked: why not using the phase angles? The answer seems to lie in the nature of the phase angle, as can be seen from Fig. 2. Small changes in phase angle are difficult to establish. The amplitudes, in contrast, have a reasonable value over much of the complete cycle, so that the average maximum amplitude A can be determined with much larger precision than the phase angles.

7. SOME REMARKS ABOUT TRANSITIONS

Transitions are of interest to thermal analysis since they indicate the limits of solids, mesophases, and liquid states. Similarly, a chemical transition is always coupled with a change in thermal parameters and can thus be followed conveniently by thermal analysis. Measuring with MDSC will, in principle, be able to register any reversible transition and ignore any irreversible, spontaneous change. The latter can, in turn, be measured by the total heat flux (see Section 2) if before and after its occurrence steady state is attained. One uses then the baseline method to bridge the time/temperature interval during which the calorimeter is out of steady state [5]. In this fashion a much better characterization of any material should be possible than by DSC alone. Complications arise, however, if the heat effect is so large that it disrupts the steady state of the MDSC, as expressed by eqns. (6), (10) and (11). Besides the interruption of steady state, one often finds that transitions are only partially reversible. Then MDSC could drive valuable information on the degree of reversibility (assuming that any deviation from steady state is negligible or can be properly assessed). In this area of separation of instrument effects due to loss of steady state and deviation from reversibility further quantitative work is necessary.

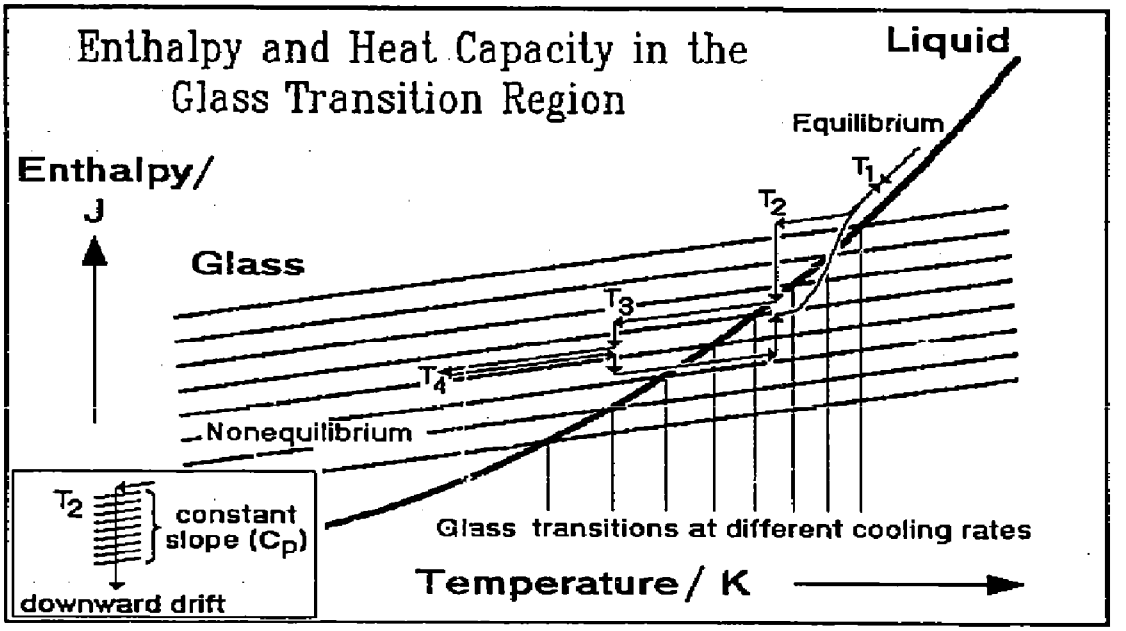

Fig. 4. Schematic diagram of the enthalpy in the glass transition region.

A qualitative analysis of the superposition of a reversible and an irreversible process is schematically illustrated in Fig. 4 for the example of the glass transition analyzed by quasi-isothermal MDSC (see Section 4). Somewhat below the glass transition temperature T_g, the heat capacity follows any change of the temperature almost instantaneously. Molecular dynamics simulations have shown that for solid polymers the time involved to reach a steady state temperature is in the picosecond range (10^{-12} s) [12]. One can thus write the solid heat capacity simply as

$$C_p(\text{solid}) = C_{p,\text{vib}} \tag{28}$$

by representing the vibrational heat capacity by $C_{p,\text{vib}}$, as it is available through the Advanced THermal Analysis System, (ATHAS) [13]. Other contributions to C_p(solid) are usually negligible. The parallel thin lines in Fig. 4 represent the enthalpies $H(=\int C_p\,\mathrm{d}T)$ of various glasses that were cooled at different rates. The higher the line, the faster was the liquid cooled through the glass transition. Once in the glassy state, all heat capacities are the same (but not the enthalpies).

In the liquid state, longer times are needed to reach thermal equilibrium because of the need of the molecules to undergo larger, cooperative, structural changes. A simple model for the representation of these motions has been given by Eyring [14a] and Frenkel [14b] in terms of a hole theory, i.e. the larger expansitivity of liquids and the slower response to external forces is said to be due to changes in a hole equilibrium. The equilibrium number of holes is N_h^*, each contributing an energy ε_h to the enthalpy. The

hole contribution to the heat capacity is then given by the change in number of holes with temperature under equilibrium conditions

$$C_p(\text{liquid}) = C_{p0} + \varepsilon_h\left(\frac{dN_h^*}{dT}\right) \tag{29}$$

Creation, motion, and destructions of holes are, however, kinetic processes and may be slow. This leads to deviations from eqn. (29) if the measurement is carried out faster than the kinetics allows. Applied to the glass transition, one can write a simple, first-order kinetics expression [15] that has been extended to describe the time-dependent, apparent heat capacity in the glass-transition region [16]

$$\left(\frac{dN_h}{dt}\right) = \frac{1}{\tau}(N - N_h^*) \tag{30}$$

with N representing the instantaneous number of holes, and N_h^*, again the equilibrium number of holes; τ is the activation energy for the formation of holes. Both N_h^* and τ are available through the hole theory [16].

Some 5 to 10 K above T_g most one phase and one component systems show no kinetic effects when heating or cooling rates are slower than about 20 K min^{-1}. The enthalpy is equal to the heavy curve in Fig. 4. On going through T_g, the glassy state is reached at different temperatures for different cooling rates, freezing-in different numbers of holes and giving rise to the multitude of glasses with different enthalpies indicated in Fig. 4. Using MDSC the slope of the enthalpy of these glassy states can be measured, irrespective of the enthalpy level. In the temperature range where modulation frequency and relaxation times are comparable, eqn. (30) must be considered.

Let us now first follow a stepwise cooling and heating experiment in which long-time quasi-isothermal MDSC experiments are carried out sequentially between T_1 and T_4. At T_1 the heat capacity is represented by eqn. (29), the modulation is slow enough to be followed by the kinetics of eqn. (30). Cooling quickly to T_2 yields initially a glass represented by the upper thin enthalpy line. At this temperature the modulation frequency is already too fast to measure anything but the heat capacity of the glass (eqn. (28)). Since the measurement is carried out over many modulation cycles, the enthalpy relaxes to lower levels of enthalpy in an irreversible process. These enthalpy changes are little affected by the small temperature oscillations, and thus not measured by MDSC. The lower left insert illustrates this downward drift that can be computed with the use of eqn. (30). Even if ultimately the equilibrium liquid were reached, as suggested in the figure, the measured heat capacity would still be that of the solid since the hole equilibrium could not be changed significantly during the

modulation period. Continuing to T_3 the enthalpy relaxation is less, but again unrecorded by MDSC. At T_4, a metastable glass has finally been reached. On reheating, the relaxations at T_3 and T_2 would, again, not be recorded. During the jump to T_1 the relaxation time is shortened sufficiently that the hole contribution can be measured and C_p is again represented by eqn. (29). On the cooling as well as on the heating run the heat capacity between T_1 and T_2 is intermediate between eqns. (28) and (29), giving a glass transition temperature at half-vitrification [17] that is governed only by the time scale of modulation. In this way MDSC is able to establish a precise (modulation time scale dependent) glass transition temperature on cooling as well as on heating. Normal DSC is unable to do the latter because of the simultaneous recording of heat capacity and enthalpy relaxation. Special methods are necessary to extract the glass transition from a DSC trace measured on heating and showing enthalpy relaxation, and even then, one can only assess the glass transition that corresponds to the prior cooling rate (thermal history) [5].

Continuous heating and cooling experiments are expected to give a continuous recording, blurred somewhat over the temperature range of modulation.

A number of details are still missing in this analysis of the glass transition and will be addressed more quantitatively in the near future [8]. The main problems and opportunities for information to be gained by MDSC of the glass transition are the need to have the instrument calibrated simultaneously for heating and cooling (to properly follow the modulation), to understand deviations of the glass transition from the simple kinetics of eqn. (30) (the inherent symmetry for approach to equilibrium from above and below the liquid enthalpy line is not in agreement with experiment), and to develop the proper description in the narrow range of temperature where the modulation time scale is similar to the relaxation time in eqn. (30).

8. CONCLUSIONS

The now commercially available MDSC has brought the method of modulation to thermal analysis for separation of signal and noise. As expected, the major influence is on quantitative use of the technique, i.e. the measurement of heat capacity. There is no doubt that in this application a major advance has occurred. For the interpretation of high-energy transitions, the technique is not yet well enough understood to enable quantitative use, but the separation of reversing components from the total measured effect yields in most applications important additional information, and it is hoped that it will take only little additional time until the limits of quantitative analysis have been established in all areas.

ACKNOWLEDGMENTS

The authors greatfully acknowledge extensive discussions with Drs. M. Reading, ICI Paints; B.S. Crow, TA Instruments; C. Schick, U. Rostock, and R. Gunther, University of Nebraska. This work was supported by the Division of Materials Research, National Science Foundation, Polymers Program, Grant DMR 90-00520 and the Division of Materials Sciences, Office of Basic Energy Sciences, U.S. Department of Energy, under Contract DE-AC05-84OR21400 with Martin Marietta Energy Systems, Inc.

REFERENCES

1 M. Reading, D. Elliot and V.L. Hill, J. Therm. Anal., 40 (1993) 949.
2 P.S. Gill, S.R. Saurbrunn and M. Reading, J. Therm. Anal., 40 (1993) 931.
3 M. Reading, Trends Polym. Sci., 8 (1993) 248.
4 M. Reading, B. Hahn and B. Crowe, US Patent 5,244,775, 1993.
5 B. Wunderlich, Thermal Analysis, Academic Press, Boston, 1990.
6 W. Hemminger and G. Höhne, Calorimetry, Verlag Chemie, Weinheim, 1984.
7 Y. Jin, A. Boller and B. Wunderlich, in K.R. Williams (Ed.), Proc. 22nd NATAS Conf., Denver, CO, 19–22 September 1993, pp. 59–64; submitted in extended form to J. Therm. Anal.
8 A. Boller, C. Schick and B. Wunderlich, in preparation.
9 Y. Jin, A. Xenopoulos, J. Cheng, W. Chen, B. Wunderlich, M. Diack, C. Jin, R.L. Hettich, R.N. Compton and G. Guiochon, Mol. Cryst. Liq. Cryst., in press.
10 B. Wunderlich, Macromolecular Physics, Vol. 2, Crystal Nucleation, Growth, Annealing, Academic Press, New York, 1976; and Macromolecular Physics, Vol. 3, Crystal Melting, Academic Press, New York, 1980.
11 B. Wunderlich, J. Therm. Anal., 32 (1987) 1949.
Y. Jin and B. Wunderlich, J. Therm. Anal. 36 (1990) 765, 1519; 38 (1992) 2257; Proc. 21st NATAs Conf. Atlanta, GA, 13–16 September 1992, pp. 151–156 (1992), Thermochim. Acta, 226 (1993) 155–161.
12 G.L. Liang, D.W. Noid, B.G. Sumpter, and B. Wunderlich, Makromol. Chem., Theory and Simulation, 2 (1993) 245–255.
13 B. Wunderlich, S.-F. Lau and U. Gaur, in B. Miller (Ed.), Thermal Analysis, Proc. 7th ICTA, Vol. II, Heyden-Wiley, Chichester, 1982, p. 950.
Yu. V. Cheban, S.-F. Lau and B. Wunderlich, Colloid Polym. Sci., 260 (1982) 9; for updates write to the corresponding author for the biannual ATHAS reports.
14 (a) H. Eyring, Chem. Phys., 4 (1936) 238.
(b) J. Frenkel, Kinetic Theory of Liquids, Clarendon Press, Oxford, UK, 1946.
15 N. Hirai and H. Eyring, J. Appl. Phys., 29 (1958) 810; J. Polym. Sci., 37 (1959) 51.
16 B. Wunderlich, D.M. Bodily and M.H. Kaplan, J. Appl. Phys., 35 (1964) 95.
17 B. Wunderlich, The Nature of the Glass Transition and its Determination by Thermal Analysis, in R.J. Seyler (Ed.) ASTM Symp. on the Assignment of the Glass Transition, Atlanta, GA 4–5 March 1993, ASTM STP 1249, Am. Soc. Testing of Materials, Philadelphia, PA, 1994.